SCEC2 Annual Report 2006

Improving Shallow S-wave Velocity in the SCEC Community Velocity Model by Microseisms

Toshiro Tanimoto (UCSB)

Shallow S-wave velocity for improving ground motion prediction

In this project, we developed a new method to constrain shallow S-wave velocity structure underneath seismic stations. The method takes advantage of three-component seismographs and judiciously selects the Rayleigh wave portion of the data. The basic steps are:

I. **Culling of Rayleigh wave portions in microseisms:** Microseisms consist of different types of phases but mainly consist of Rayleigh waves. Figure 1 shows an example of microseismic energy between 0.1 and 0.3 Hz at Glamis (GLA); the majority of energy in microseisms display 90-degree phase shift between horizontal and vertical components. We can create a data set which is dominated by Rayleigh waves by selecting data using this pahse shift information.

II. **Measurement**: The ratios of horizontal to vertical amplitude can be measured for selected Rayleigh wave data. This can be done for the frequency range 0.1-0.2 Hz because microseism energy is abundant in that range for Southern California. Within this frequency band, 0.1-0.2 Hz, we can measure H/V and estimate their errors. In Figure 6, the top-right panel shows data (small circles) and error bars. They are estimated at every 0.05 Hz interval for three stations (Glamis GLA, Goldstone GSC and Pasadena PAS).

III. **The initial model**: We used SCEC CVM3.0 as the starting model for this preliminary study. It is a good model but in many areas, especially outside the basin regions, shallow structures are not well constrained. Therefore, theoretical H/V values for many stations are systematically off from our measured H/V. The same panel (Figure 2, top-right) shows theoretical values for SCEC CVM3.0 by dash lines and they are all shifted toward lower values at three stations. Clearly, there is room for improvement in this model.

IV. **Depth sensitivity kernels:** In order to improve the fit for H/V data, we developed a method to compute depth sensitivity kernels for H/V. In principle, perturbation to H/V is related to density, P-wave velocity and S-wave velocity (under a station) by a formula given below where η is the H/V ratio and d indicates perturbation. This is very similar to phase and group velocities that have been inverted for S-wave structure.

$$\frac{\delta\eta}{\eta} = \int \{K_\rho \frac{\delta\rho}{\rho} + K_P \frac{\delta Vp}{Vp} + K_S \frac{\delta Vs}{Vs}\} dr$$

V. **Results:** Final S-wave velocity models for the three stations are shown in the bottom panel in Figure 6. In this panel, the SCEC CVM 3.0 is shown in dashed lines and five derived models are shown in solid lines. The five models differ but they overlap in this scale of plot. Major deviations from the starting model are found near the surface, where the reduction of S-wave velocity is required. Results from three other stations are given in Figure 3. In all cases, it seems clear that SCEC CVM 3.0 requires some modifications to shallow S-wave velocity structure. We have now performed inversions for about 70 stations and expect to work on all Southern California stations soon.

This method will provide important point-wise constraint on seismic structure at each seismic station. We have started to examine an alternative approach using the noise-correlation method, which will give us phase velocity maps in the same frequency band and complement this approach. We expect to combine the two approaches and obtain reliable shallow S-wave velocity structure in coming years which will be an important input for any ground motion prediction program.

The basic methodology was recently published in Tanimoto and Alvizuri (2006) and the method is now being applied to various regions including Kanto (Tokyo) region in Japan.

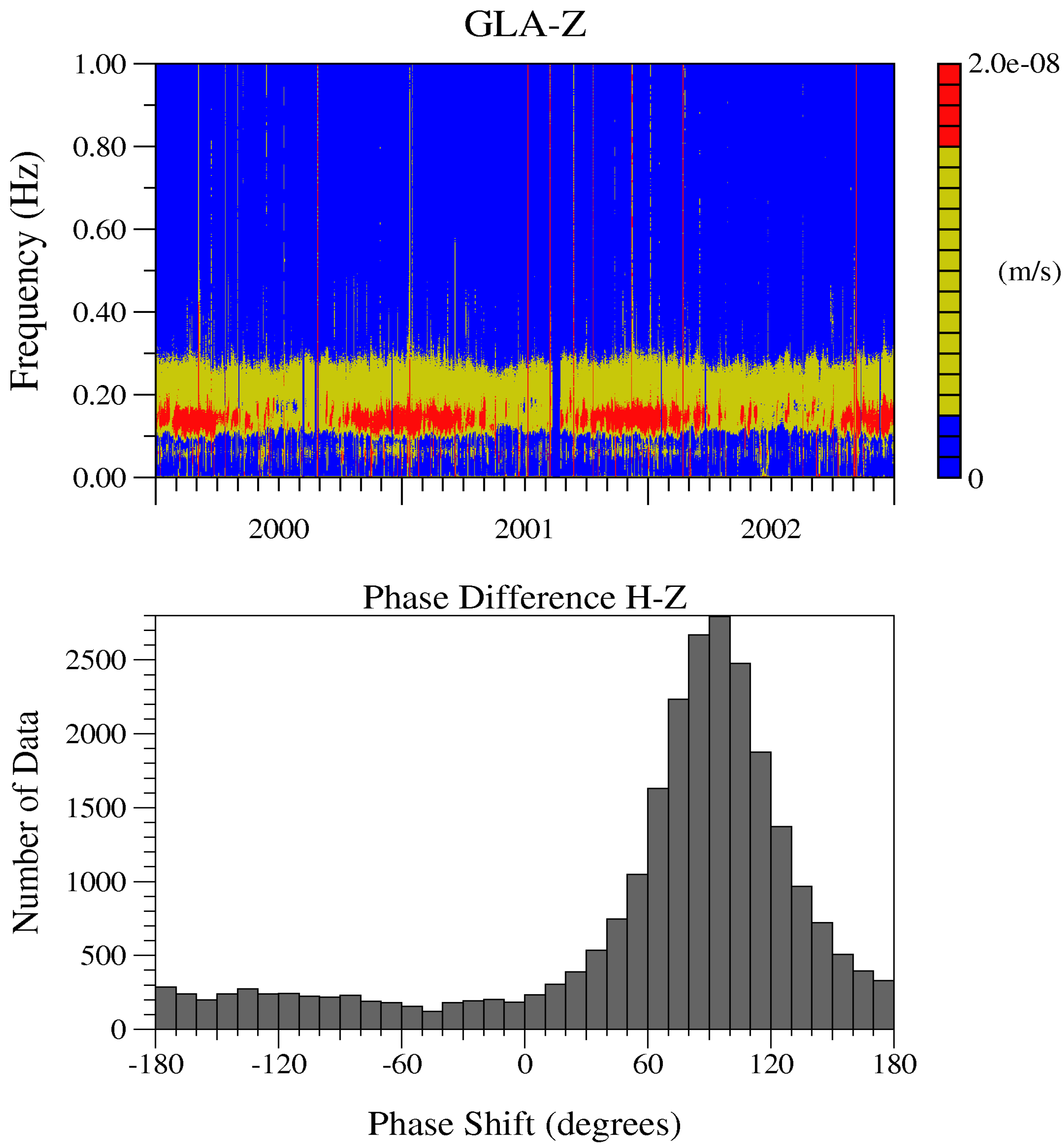

Figure 1: (Top) Vertical spectral amplitudes at Glamis (GLA) for three years. The maximum amplitudes are found at about 0.14-0.15 Hz and changes in color (red and yellow) indicate seasonal variations in source strength. (Bottom) Phase shift between horizontal and vertical components. The peak at 90 degrees indicates the retrograde particle motion and thus the dominance of Rayleigh waves in microseisms. We can cull Rayleigh wave data by selecting data near this peak.

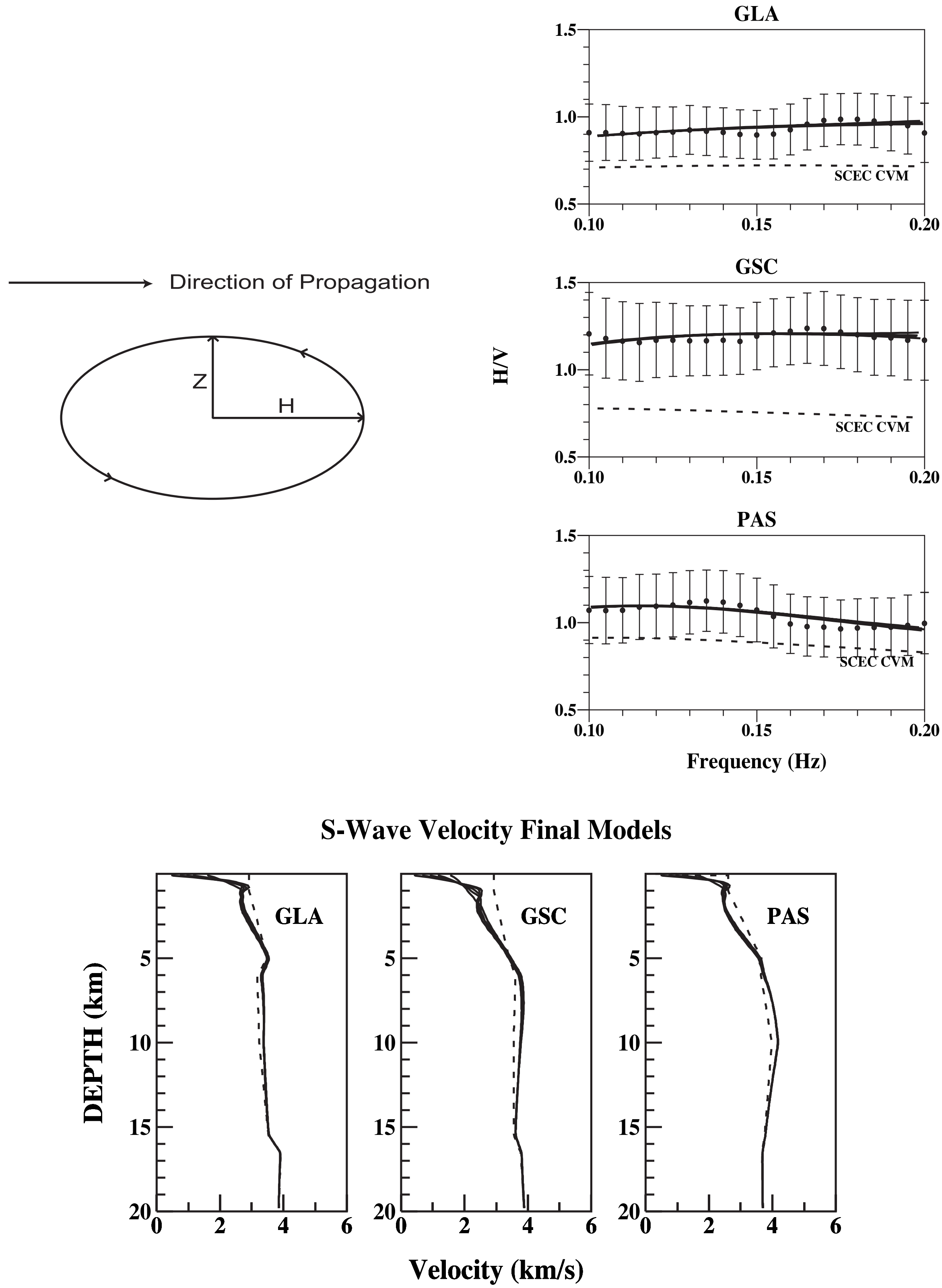

Figure 2: (Top) Fit to H/V data at GLA, GSC and PAS. The values for the initial model SCEC CVM3.0 are shown by dash. Fit for five different models are shown by five solid lines (which overlap). (Bottom) Derived S-velocity models that correspond to the fits in the top panel. Introduction of slow velocity layers at top is the main change from SCEC CVM 3.0 (dash).

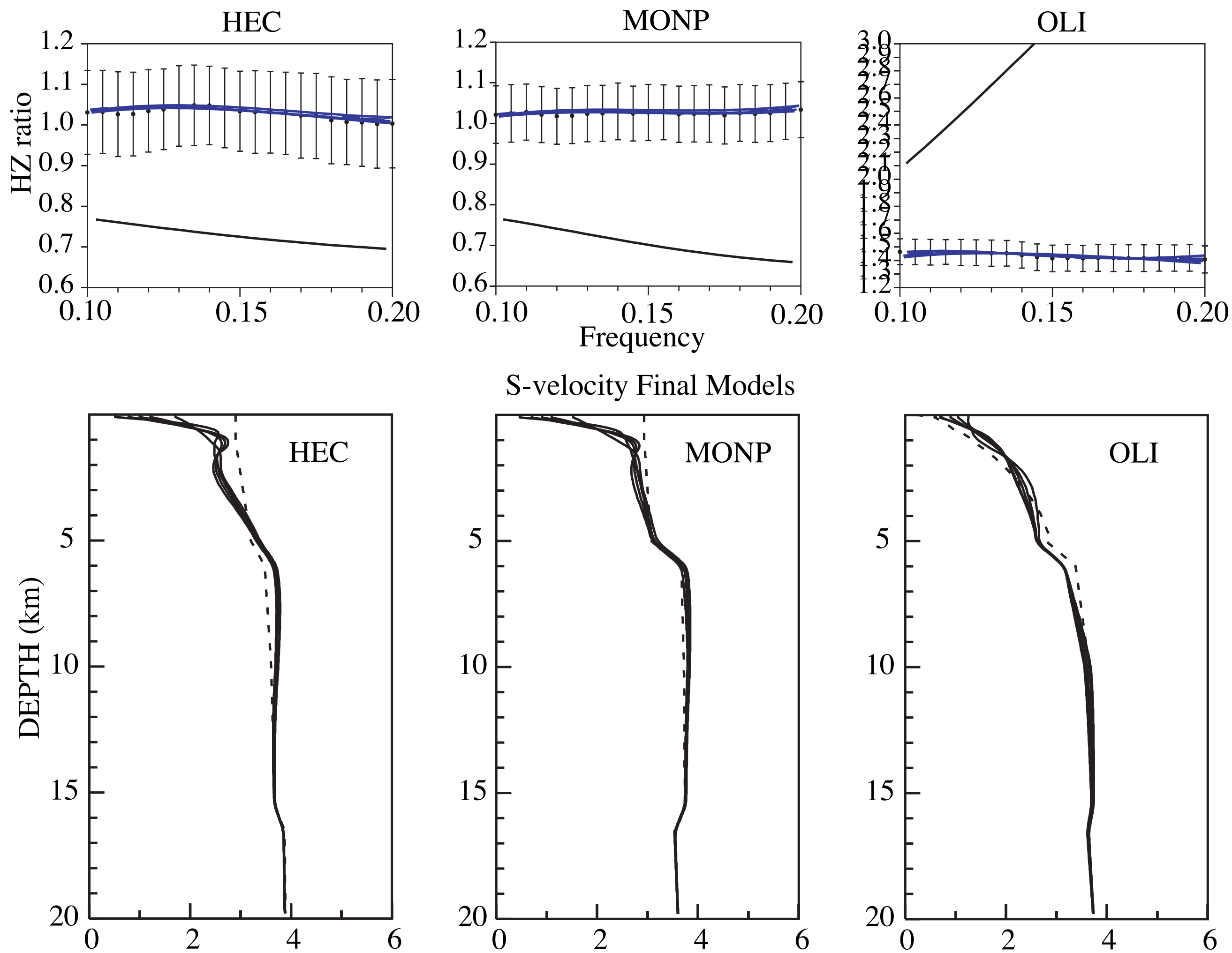

Figure 3: (Top) H/V of the initial S-wave velocity model (dash, SCEC CVM3.0) and five final models (solid) are shown with error bars derived from microseisms. (Bottom) Comparison of SCEC CVM 3.0 (dash) and five inverted models (solid). Devitations in H/V data by the initial model are mainly because of the lack of thin slow velocity layer near the surface. Stations in the basins like OLI are different in the sense that perturbations to the model are small. Large deviations in H/V data at OLI occur because vertical amplitudes at this station are very small and H/V becomes very sensitive to noise in vertical components.

List of Publication

(1) Tanimoto, T. and K. Prindle, Three-dimensional S-wave velocity structure in Southern California, Geophysical Research Letters, 29, No.8, doi:10.1029/2001GL013486, 2002. SCEC contribution number #1056

(2) K. Prindle, C. Marcinkovich, and Toshiro Tanimoto, Regional Wavefield reconstruction for teleseismic P-waves and Surface Waves, Geophysical Research Letters, vol. 29, No. 11, doi:10.1029/2001GL013721, 2002. SCEC contribution number #1057.

(3) Tanimoto, Toshiro, Geometrical approach to surface wave finite frequency effects, Geophysical Research Letters, Vol. 30, N0. 19, doi:10.1029/2003GL017475, 2003, SCEC #747

(4) Tanimoto, Toshiro, The azimuthal dependence of surface wave polarization in a slightly anisotropic medium, Geophysical Journal International, 156, 73-78, doi:10.1111/j.1365-246X.2004.02130.x, SCEC #748

(5) Tanimoto, Toshiro and L. Rivera, Prograde Rayleigh Wave particle motion, Geophysical Journal International, 162, 399-405, doi: 10.1111/j.1365-246X.2005.02481.x, SCEC #899.

(6) Tanimoto, Toshiro, S. Ishimaru, C. Alvizuri, Seasonality in particle motion of microseisms, Geophysical Journal International, 166, 253-266, doi: 10.1111/j.1365-246X.2006.02931.x, SCEC #900

(7) Tanimoto, Toshiro and C. Alvizuri, Inversion of the HZ ratio of microseisms for S-wave velocity in the crust, Geophysical Journal International, 165, 323-335, doi: 10.1111/j.1365-246X.2006.02905.x, SCEC #901

(8) Tanimoto, Toshiro, and K. Prindle, Surface wave analysis with beamforming, Geophysical Journal International, submitted 2006, SCEC #1037.

(9) Prindle, K. and T. Tanimoto, Teleseismic surface wave study for S-wave velocity structure under an array: Southern California, Geophys. J. Int., 166, 601-621, doi:10.1111/j.1365-246X.2006.02947.x, 2006, #936